Secoisolariciresinol diglucoside reduces cell death and upregulates antioxidants in cardiac iron overload

A thesis presented to

The Faculty of Graduate Studies

of

Lakehead University

by

Ashley Nemec-Bakk

In partial fulfillment of requirements

for the degree of

Master of Science in Biology

September 27, 2016

Abstract

Iron is essential to many biological and metabolic processes used in all organisms, but excess iron can result in complications such as cirrhosis, diabetes, and heart failure. Cardiac iron overload has been linked to increased oxidative stress and cell death. Oxidative stress has been shown to play a role in cardiovascular diseases. Antioxidants can counter the effect of oxidative stress by scavenging reactive oxygen species. Protein kinase B (Akt) promotes cell survival by regulating growth, antioxidant production, and cell death in cardiomyoctes. The aim of this study was to examine the cardioprotective role of secoisolariciresinol diglucoside (SDG), a phytochemical extracted from flax seeds, in an *in vitro* cardiac iron overload condition. H9c2 cardiac cells were incubated with 50 μM iron for either 6, 12 or 24 hours and/or received a SDG pretreatment of 250 μM or 500 μM for 24 hours. Flow cytometry was used to assess necrotic cells and changes in the mitochondrial membrane potential. Western blot was used to determine the protein expression of antioxidants (manganese superoxide dismutase and catalase) and redox sensitive proteins, 5'AMP-activated protein kinase (AMPK), signal transducer and activator of transcription 3 (STAT3), Akt, and the mammalian target of rapamycin (mTOR). Pretreatment of SDG reduced the amount of necrotic cells (24.3%) after iron treatment. Pretreatment of SDG resulted in increased protein expression of catalase after 24 hours of iron treatment, and increased activity of AMPK and STAT3 after 12 hours of iron treatment. Akt activity and 4-hydroxynonenal (4HNE) levels were decreased after 6 hours of iron treatment when pretreated with SDG. This study demonstrates that SDG can act as an antioxidant by attenuating cell death, oxidative stress, and increasing the level of intrinsic antioxidants.

Lay Summary

Faculty and students in the Department of Biology are bound together by a common interest in explaining the diversity of life, the fit between form and function, and the distribution and abundance of organisms. This research project focussed on the field of human sciences and investigated the mechanism behind the antioxidant activity of secoisolariciresinol diglucoside (SDG) in an *in vitro* cardiac iron overload model. The findings suggest SDG protects cardiomyocytes from iron overload by increasing antioxidant levels and pro-survival proteins. SDG may be a therapeutic option for patients with iron overload condition.

Acknowledgements

I would like to thank my mentor and supervisor Dr. Neelam Khaper for her guidance and support throughout my Masters. I would also like to thank my committee members Dr. Simon Lees and Dr. Heidi Schraft for providing me with helpful advice throughout my thesis. I would also like to thank Dr. Stephanie Puukila and Heidi Forsyth for teaching and helping me with my experiment over the years, as well as Stefanie Kirk for helping with this project. I would also like to thank Ontario Graduate Scholarship (OGS) and Lakehead university for providing me with funding during my Master's program. Finally, thank you to all the research students at the Northern Ontario School of Medicine laboratory for the positive working environment and fun memories.

Abbreviations

Akt - Protein Kinase B

AMPK - Adenosine monophosphate-activated protein kinase

Atg - Autophagy protein

ATP - Adenosine triphosphate

Bax - B-cell lymphoma-associated X protein

Bcl - B-cell lymphoma

ED - Enterodiol

EL - Enterolactone

Fe^{3+} - Ferric

Fe^{2+} - Ferrous

FOXO - Forkhead box subfamily O

GPx - Glutathione peroxidase

GSH - Glutathione

H_2O_2 - Hydrogen peroxide

HSP - Heat shock protein

IL - Interleukin

$^{\cdot}OH$ – Hydroxyl radical

LDL - Low-density lipoprotein

mTOR - Mammalian target of rapamycin

mtDNA - Mitochondrial DNA

mPTP - Mitochondrial permeability transition pore

SOD2/MnSOD - Manganese superoxide dismutase

MI - Myocardial infarction

NTBI - Non-transferrin bound iron

LTCC - L-type Ca^{2+} channels

PI3K - Phosphoinositide 3-kinase

ROS - Reactive oxygen species

SECO - Secoisolariciresinol

SDG - Secoisolariciresinol diglucoside

STAT - Signal transducer and activator of transcription

$O_2^{\circ-}$ - Superoxide anion

SOD - Superoxide dismutase

TNF-α - Tumor necrosis factor-alpha

Table of Contents

List of figures

Introduction

1.0 Iron Overload

Iron is essential to biochemical, metabolic, and biological processes in all organisms, where it is the critical component of haemoglobin and is needed for energy production (1). The biological importance of iron and its toxicity is a result of rapid oxidation-reduction cycling between ferric (Fe^{3+}) and ferrous (Fe^{2+}) states at physiological conditions (2). Therefore, iron is precisely regulated under physiological conditions by several intrinsic feedback mechanisms that utilize transporters, iron-binding proteins and receptors (2). However, an excess of iron can result in complications such as heart disease, cirrhosis, and diabetes (1). Iron overload occurs when the amount of free iron exceeds the capacity of iron binding to serum transferrin (1). This excess iron results in highly reactive non-transferrin-bound iron (NTBI) which can bypass the negative-feedback mechanisms regulating cellular iron uptake (2). Excess NTBI uptake combined with the lack of an effective iron excretory pathway leads to the expansion of the labile intracellular iron pool as well as the formation of reactive oxygen species (ROS) which results in lipid peroxidation and oxidative damage to proteins (2). Excess iron can accumulate in the liver, spleen, heart, and central nervous system (3). Cardiac iron overload is caused by the accumulation of iron in the myocardium and is the leading cause of death in patients receiving chronic blood transfusion therapy (3). One unit of transfused blood contains about 250 mg of iron and over long periods of repeated blood transfusions iron is deposited into multiple organs leading to iron overload (3). Chronic cardiac iron overload can lead to a variety of arrhythmias which can lead to heart failure

(1). Recent studies have suggested that altered calcium homeostasis and increased production of ROS each play a role during cardiac iron overload (1, 2).

1.1 Iron overload conditions

Primary hemochromatosis is a common inherited disorder where excessive iron accumulation results primarily from increased gastrointestinal absorption of iron and modified environmental factors (2). Secondary hemochromatosis occurs in patients with hereditary anemias including thalassemia and sickle cell anemia (2). α- and β-thalassemia's are caused by mutations resulting in defective synthesis of the α- and β-globulin chains of hemoglobin and are the most common monogenetic diseases in humans (2). Secondary iron overload can occur after repeated blood transfusions coupled with increased gastrointestinal absorption, which leads to symptoms similar to primary iron overload (2). To prevent iron accumulation caused by blood transfusions the use of chelation therapy is required at the beginning of the transfusions or phlebotomy (4).

1.2 Cardiac iron overload

Cardiac iron overload is a common cause of cardiovascular deaths worldwide (5). In patients with hemochromatosis or thalassemia major cardiovascular disease contributes significantly to their mortality and morbidity (2). Cardiac iron overload has been shown to lead to restrictive cardiomyopathy with prominent early diastolic dysfunction that progresses to dilated cardiomyopathy characterized by impaired systolic function often accompanied by arrhythmias and sudden cardiac death (1-3). Iron overload in the heart may also facilitate myocardial ischemia-reperfusion injury because of an increased formation of ROS and reduced antioxidant defenses (Figure 1) (2). During the

advancement of cardiac iron overload, iron accumulates in the ventricular wall, the epicardium, the papillary muscles, and septum (6). Although the exact mechanism of iron induced cardiomyocyte dysfunction is not fully understood, recent studies suggest that generation of free radicals plays an important role (1-2, 6).

1.3 Iron transport

The human body uses about 20mg of iron per day for hemoglobin synthesis and 4-5mg for the production of cellular proteins and approximately 200 billion erythrocytes (2). Most of the iron in the body is contained in hemoglobin but it can also be stored in hepatocytes and macrophages as ferritin (2, 7). Iron is delivered to most cells through the blood as ferric iron bound to serum protein transferrin which is relatively nonreactive (7). Movement of iron within the body involves a combination of transporters, including transferrin receptors, dimetal transporter 1, ferroportin and a heme receptor (2). Ferroportin exports reduced iron into the plasma where it is oxidized and binds to transferrin (2). Iron can also be imported as a heme-iron complex into selected tissues (2).

Recently it has been suggested that L-type Ca^{2+} channels (LTCC) are responsible for the transport of NTBI into the cell (2). Excitable cells and tissues with the greatest risk in iron overload have high LTCC activity, which supports the idea that LTCC's are responsible for cellular uptake of NTBI (2). LTCCs are the only Fe^{2+} transporter whose activity increases with elevated iron, which is consistent with NTB1 uptake in the heart under iron overload conditions (2). Studies with mice using LTCC blockers, amlodipine and verapamil, demonstrated reduced intracellular myocardial iron accumulation and oxidative stress while preserving cardiac function (2).

1.4 Treatment

There are two treatments available for patients suffering from iron overload, phlebotomy and chelation therapy. However, both treatments have been shown to have adverse side effects. Phlebotomy is the removal of blood from the body and patients receiving phlebotomy can live a normal lifespan if treatment is started early (8). Chelators when injected into the bloodstream bind and remove metals from the body (8). Chelation therapy has been shown to improve ventricular function, prevent ventricular arrhythmias and reduce mortality in patients with secondary iron overload (8). Phlebotomy may still result in cardiac iron overload and chelation therapy may cause toxic side effects including agranulocytosis, gastric intolerance, and zinc deficiency limiting its clinical use (8).

2.0 Oxidative Stress

Numerous studies have shown that oxidative stress is involved in the pathogenesis of many cardiovascular diseases such as hypertension, type II diabetes, atherosclerosis and heart failure (9). Under baseline conditions, ROS are produced in the mitochondria during aerobic respiration (10). Vascular cells produce large amounts of ROS including superoxide ion ($O_2^{\bullet-}$), hydrogen peroxide (H_2O_2), the hydroxyl radical and a range of lipid radicals (9). $O_2^{\bullet-}$ is a primary species involved and can form other ROS as a consequence of biochemical reactions (9). The main sources of ROS in cardiovascular tissues are NAD(P)H oxidase, xanthine oxidase, uncoupled endothelial nitric oxide synthase and the mitochondrial respiratory chain (9).

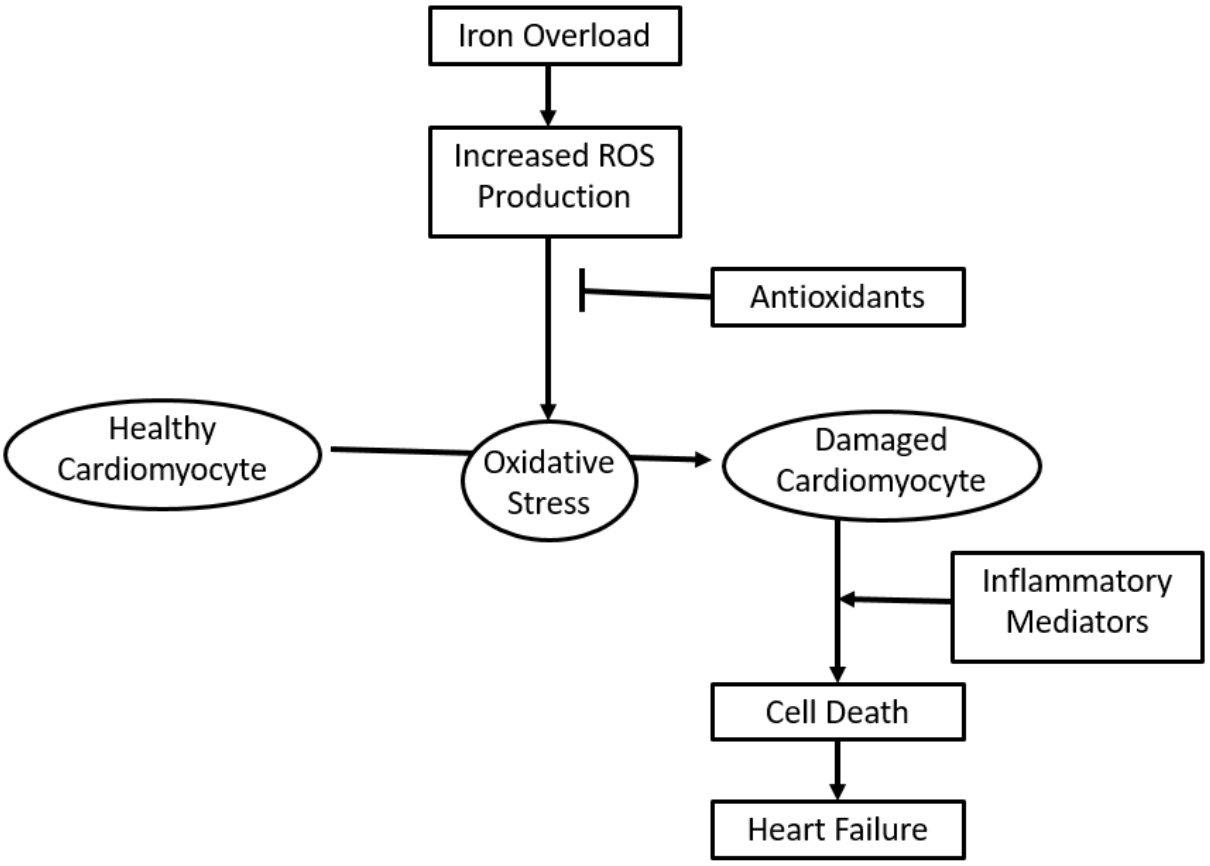

Figure 1: Iron induced cardiac damage. Schematic illustration of iron induced oxidative stress in cardiac cells. Image modified from Gammella et al (2015) (53).

2.1 Antioxidant defense system

The production of ROS is equalized by enzymatic and non-enzymatic antioxidants such as superoxide dismutase (SOD), catalase, glutathione peroxidase (GPx), thioredoxins, peroxiredoxins, and ascorbic acid which act as ROS scavengers (Figure 2) (12, 13). The contribution of metal ions to ROS generation is most common in Fenton or Fenton-type reactions where endogenous metals, such as Fe^{2+} and Cu^{+}, react with hydrogen peroxide to generate hydroxyl radical (13). The cytotoxicity of superoxide radical is diminished by SOD that catalyzes the reduction of $O_2^{\bullet-}$ to H_2O_2 and O_2 (13). Three different isoforms of SOD have been identified in humans and contain copper, zinc or manganese ions in their active sites (13). The protective effects of SOD have been demonstrated in animal models where SOD significantly protects the heart and brain from ischemic injury and prevents alcohol-induced liver injury (13). Antioxidant enzymes such as catalase and GPx scavenge H_2O_2 by reducing it to H_2O (13). Catalase is located in the peroxisome and its function is to promote the conversion of H_2O_2 to water and molecular oxygen (14). GPx enzymes in the presence of tripeptide glutathione (GSH) will add two electrons to convert peroxides to water while oxidizing GSH (Figure 2) (14). These antioxidant enzymes eliminate peroxides as potential substrates for the Fenton reaction (14). The reduction of H_2O_2 by metal ions generates the hydroxyl radical, which is considered to be the most reactive ROS (13). The Fenton reaction occurs when iron reacts with endogenous H_2O_2 to generate OH^- and $OH^{\bullet}$ (13). Copper generates hydroxyl radical in a Fenton-type reaction 50 times faster than with iron (13).

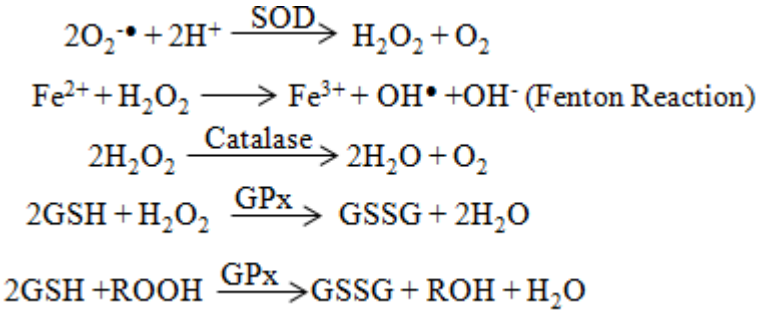

Figure 2: Antioxidants and free radicals. Redox reactions illustrating the production of some ROS and the antioxidants involved in scavenging the free radicals. Image modified from Flora (2009) (14).

2.2 Oxidative stress mediated cell damage

2.2.1 Apoptosis

Apoptosis is a form of programmed cell death (10, 11). Apoptosis is an early event in both inflammatory-mediated and mechanical injury (11). Release of cytokines such as TNF-α (tumor necrosis factor) after sepsis, ischemia-reperfusion, or shock contributes to endothelial apoptosis (10, 11). ROS has been shown to initiate apoptosis (10, 11). DNA damage is prominent in the presence of excess ROS, with mitochondrial DNA (mtDNA) being highly susceptible to ROS-mediated damage, due to its close proximity with the major source of ROS within the cell (10). Oxidative stress can cause DNA damage by binding to DNA forming adducts or by causing single or double-stranded breaks in nuclear DNA (10). ROS also causes protein damage which occurs via formation of protein carbonyls in several cellular proteins in their amino acids, lysine, arginine, proline and threonine (10). Bax/Bak is a pro-apoptotic protein of the Bcl-2 family that are negatively regulated by Bcl-2 (22). Oligomerization of Bax/Bak proteins

is believed to form ion conductance channels which alter the permeability of the mitochondrial membrane (16). Loss of membrane integrity promotes the release of pro-apoptotic factors located between the matrix and inner membrane space (16). ROS also modulates several lipoproteins, such as LDL, and causes lipid peroxidation (10). Damage to extracellular lipids is demonstrated by the accumulation of oxidized LDL, leading to the formation of foam cells from macrophages which contribute to the progression of atherosclerosis (10). Oxidation of cellular membrane systems results in altered fluidity and membrane damage (10). Cardiac iron overload has been shown to cause apoptosis resulting in loss of cardiomyocytes (2). Amplified apoptosis and/or necrosis may be due to mitochondrial dysfunction caused by iron induced oxidative stress (2).

2.2.2 Necrosis

Necrosis is a form of programmed cell death that is associated with oxidative stress, and triggers distinct changes in cell morphology distinguishing it from apoptosis (16). Permeability changes in the inner mitochondrial membrane, typically from the presence of ROS, resulting in the formation and opening of the mitochondrial permeability transition pore (mPTP) is a primary characteristic of necrosis (16). Studies suggest that the mPTP opening of the mitochondrial pore may activate apoptosis when ATP levels are maintained but a severe decline in ATP triggers necrotic cell death from a loss of electrochemical gradient across the inner mitochondrial membrane (16). Consequential swelling of the inner mitochondrial membrane leads to the rupturing of the outer mitochondrial membrane, releasing mitochondrial proteases into the cytoplasm

(16). The release of enzymes and proteins induces an inflammatory response by nearby cells which is another distinct feature of necrosis (16).

2.2.3 Autophagy

Oxidative stress has been shown to stimulate autophagy during periods of nutrient deprivation, ischemia/reperfusion and hypoxia (10). Under physiological conditions, autophagy is a constant, cytoprotective pathway used by eukaryote cells to degrade and recycle cellular components, including aged proteins and damaged organelles (20, 21). Recent evidence has shown that under baseline conditions autophagy is an important homeostatic mechanism for maintaining normal cardiovascular function (21). Enhancement of autophagy has been observed in developing mouse embryos, suggesting that autophagy plays an important role in cell development and differentiation (17). Autophagy is also up-regulated during periods of cellular starvation as a means to generate the nutrients to sustain cell survival (17-19). Therefore, autophagy is thought to be involved in many physiological processes, including cellular differentiation, tissue remodelling, and modulating growth (21, 22). Autophagic degradation and removal of damaged oxidized proteins in response to oxidative stress has been shown to benefit the cell (17). Conversely, excessive induction of autophagy by severe oxidative stress may activate signaling pathways that have a role in cardiomyopathy (17, 20, 21). During ischemia, the resulting decrease in ATP generation results in the phosphorylation of AMP-activated protein kinase (AMPK), which results in autophagosome formation through inhibition of the mammalian target of rapamycin (mTOR) (17). Ischemic insult also results in phosphorylation of heat shock protein (Hsp)20 at serine residue 16, leading

to cardioprotection by enhancing autophagy (17). During reperfusion, ROS enhances autophagy by damaging organelles, cytosolic proteins and causes lipid peroxidation in the mitochondria (17). Antioxidants such as catalase and SOD are targeted by autophagosomes, thereby increasing the presence of ROS and creating a positive feedback loop which leads to cell death (17). AMPK activity is also decreased during reperfusion, thus increasing autophagic death and beclin-1 upregulation (17).

3.0 AMPK Signaling

AMPK is a sensor of cellular energy status and plays an important role in modulating energy metabolism and ROS regulation (23-25). Due to its homeostatic activity, AMPK is being considered as a possible therapeutic target for many pathophysiological conditions including diabetes, obesity, and cardiomyopathy (23-24). These diseases are associated with chronic ROS accumulation which links to an insensitivity of AMPK activation (23). AMPK is known to be activated during stress conditions such as starvation, hypoxia, and ischemia (26). Upon energy exhaustion, AMPK stimulates ATP-production pathways while inhibiting ATP-consuming pathways, thereby regulating metabolic processes towards cellular energy homeostasis (26). Glucose deprivation in cardiomyocytes induces autophagy via activation of AMPK (26). Glucose deprivation has been shown to increase AMPK phosphorylation and decrease mTOR phosphorylation (28). The mTOR-dependent signaling pathway, which phosphorylates and inhibits the ULK1 kinase complex, regulates the induction of autophagy through AMPK (23, 28). Compromised cellular energy production inhibits mTOR through activation of AMPK and consequently, phosphorylation of the tuberous

sclerosis complex (TSC) (25, 28). TSC2 inhibits mTORC1 leading to a decrease in protein synthesis and cell growth (27). mTOR can also be inhibited directly by AMPK by directly phosphorylating the rotor compartment of mTOR (Figure 3) (27). Since mTOR negatively regulates autophagy, this pathway may be important in regulating cell death in pathological conditions (25). In cardiac muscle, insulin antagonizes the activation of AMPK and this appears to involve activation of the protein kinase B (Akt) (Figure 3) (28). Phosphorylation of AMPK at residues Ser485 and Ser491 by Akt provokes AMPK activation via phosphorylation at Thr173 by LKB1 kinase (28). mTOR was shown to be associated with the mitochondrial outer membrane, thereby sensing changes in the ratio between ATP/AMP controlling autophagy (28). mTOR also regulates the ubiqiotination, internalization and turnover of specific nutrient transporters (31). mTORC1 can regulate the trafficking of nutrient transporters and promote the uptake of various nutrients including glucose, amino acids and iron (31). Akt is a major effector of receptor tyrosine kinases, which modulate cell growth, apoptosis, protein synthesis and energy metabolism (30).

AMPK also regulates p53 expression and phosphorylation (29). During stress conditions, the p53 pathway suppresses the AKT and mTOR pathways and promotes the induction of apoptosis (29, 31). AMPK activity is increased during stress signals and negatively regulates the IGF-I-Akt-mTOR pathways in a p53-dependent fashion (29). p53 has been shown to regulate autophagy directly through its transcription regulation of damage-regulated autophagy modulator, which is a lysosomal protein (31). Akt inhibits apoptosis through inactivation of the proapoptotic factors BAD and procaspase-9 (30). Akt also phosphorylates and inhibits the TSC1/TSC2 protein complex, leading to

activation of mTOR which in turn upregulates cell growth and protein synthesis (30). Translocation of Akt from the plasma membrane to the nucleus results in the phosphorylation of FOXO transcription factors (31). FOXO proteins then exit the nucleus resulting in a transcriptional program that enhances oxidative phosphorylation for efficient energy production, increasing production of antioxidants, and heat shock proteins (31). Therefore, removal of FOXO from the nucleus by the translocation of Akt to the nucleus results in reduced apoptosis and encourages cells into cell cycle (31).

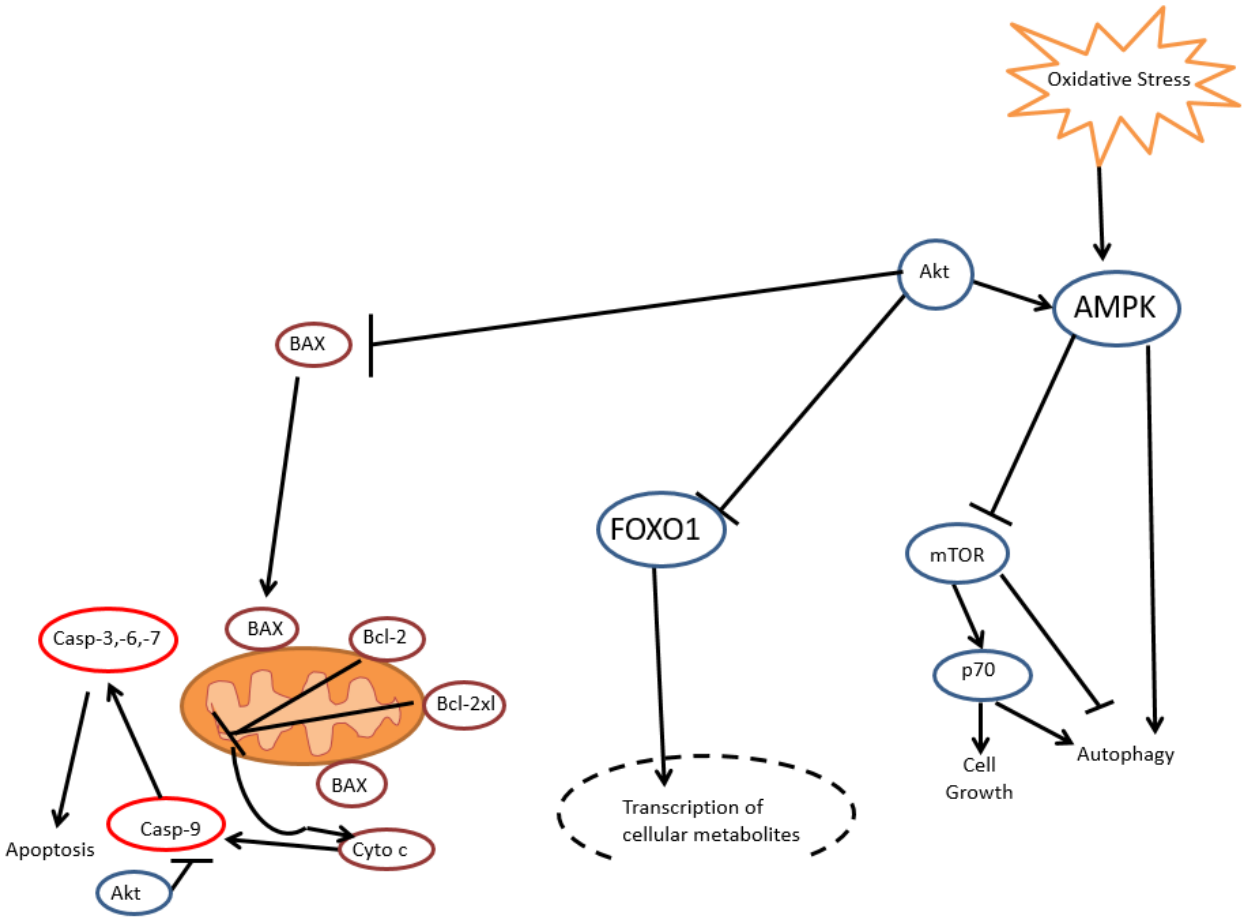

Figure 3: Akt/mTOR signaling pathway. Schematic illustration of apoptosis and prosurvival signaling pathways. Image modified from Carnero et al (2008) (52). *AMPK* 5'AMP-activated protein kinase, *Akt* protein kinase B, *mTOR* mammalian target of rapamycin, *FOXO1* forkhead box O1, *BAX* BCL2 associated X protein, *BCL* B-cell lymphoma, *Casp* caspase, *Cyto C* cytochrome c.

4.0 STAT3 signaling

Signal transducer and activator of transcription 3 (STAT3) protein is involved in cardiomyocyte protection and hypertrophy (37). STAT3 is involved in a broad range of cellular and molecular pathways that direct remodeling processes in cardiac physiology and pathophysiology (37). It can act as a signaling molecule, transcription factor and has recently been identified as a mitochondrial protein involved in energy production (37). Cytokines of the interleukin-6 family are activated via their common receptor gp130, that subsequently forms homo- or heterodimers, STAT3 then translocates to the nucleus where it activates the transcription of downstream target genes by binding to specific DNA elements in their promoter regions (37). Activation of STAT3 by the gp130 receptor system involves the constitutive assembly of JAK and tyrosine and their catalytic activation, leading to a phosphorylation of C-terminal tyrosine residues in the intracellular domain of the gp130 receptor (37). After detachment from the receptor, phosphorylation of STAT permits the homo- or heterodimerization of STAT proteins and their importation into the nucleus where it immediately activates its target genes (37). STAT3 has been shown to repress the expression of p53 and thereby down regulates pro-apoptotic genes including Bax, caspase 6, and FAS (37). In the heart, cardioprotective effects of STAT3 have been linked to a direct transcriptional up-regulation of antioxidant enzymes such as MnSOD, as well as the induction of anti-apoptotic Bcl-xL and Hsp70 (37). Therefore, STAT3 seems to contribute to the antioxidant defense mechanisms and additional cytoprotective pathways, thereby playing an important role in cardiomyocyte survival.

5.0 Secoisolariciresinol diglucoside

Secoisolariciresinol diglucoside (SDG) is a phytochemical antioxidant present in flaxseeds (32). SDG is converted to mammalian lignans after ingestion and further undergoes hydrolysis to secoisolariciresinol (SECO) (34). SECO is then converted to enterodiol (ED) and enterolactone (EL) which have a similar structure to oestradiol, the active form of oestrogen (Figure 4) (34). Their structural similarities allow ED and EL to bind to oestrogen receptors and exert weak oestrogenic effects including the induction of phase 2 proteins (oxidant scavengers) and inhibition of enzymes such as 5α-reductase and aromatase which may result in protection against chronic diseases (34). SDG has been shown to reduce the production of inflammatory mediators and oxidative stress markers in rabbits fed a high cholesterol diet and in an *in vitro* cardiac iron overload condition (32-33). SDG treatment was also found to reduce the development of atherosclerosis and diabetes in rats (32). Prasad (1997) demonstrated that SDG has an ability to scavenge OH radical therefore exhibiting antioxidant properties (35).

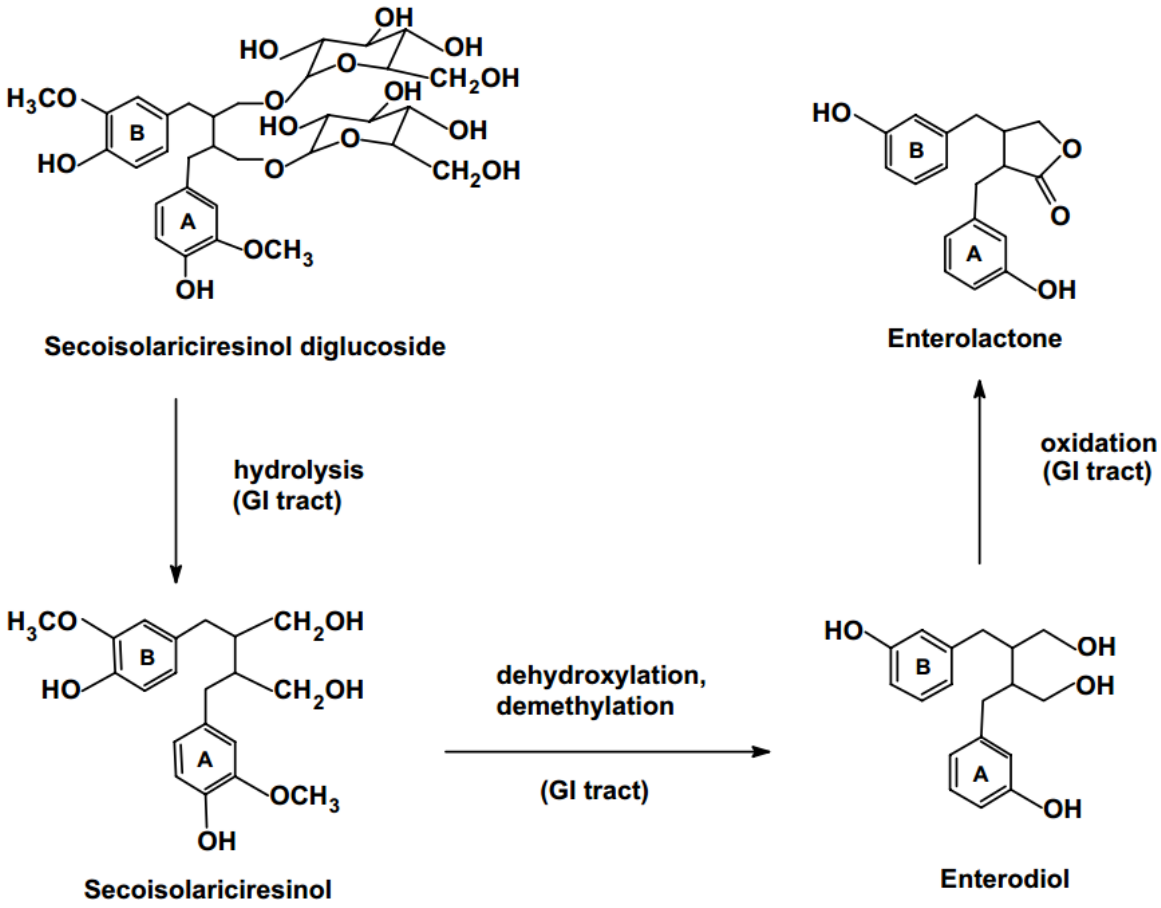

Figure 4: Structure of SDG metabolites. Demonstrates the conversion of SDG to it's metabolites EL and ED. Image from Hu, C et al (2007) (36).

6.0 Objectives

The purpose of this study was to explore SDG's role in the AMPK signaling pathway and to also investigate its effect on antioxidant protein expression, MnSOD and catalase, in a cardiac iron overload condition. Another objective of this study was to determine if SDG pretreatment would attenuate cell death and damaged mitochondria during iron induced oxidative stress.

7.0 Hypothesis

In this study we hypothesize that SDG will increase the activity of the pro-survival proteins AMPK, mTOR, Akt, while maintaining endogenous antioxidants catalase and MnSOD. SDG will also reduce the amount of necrotic cells caused by oxidative stress in an *in vitro* cardiac iron overload condition.

Methods

Cell culture

Rat ventricle cardiac cells, H9c2 cells (American Type Culture Collection, Manassas, VA), were grown in Dulbecco's Modified Eagle's Medium (DMEM) (Sigma-Aldrich, St. Louis, MO) supplemented with 10% (vol/vol) fetal bovine serum (Hyclone, Pittsburgh, PA) and 1% penicillin-streptomycin (Invitrogen, Carlsbad, CA) in a humidified atmosphere containing 5% CO_2 at 37°C. Cells were grown to 80% confluency before treatments. All experiments were conducted in the absence of serum and antibiotics.

Ammonium iron (III) citrate preparation

Iron solution was prepared by dissolving ammonium iron (III) citrate (Sigma-Aldrich, St. Louis, MO) into serum- and antibiotic-free DMEM. H9c2 cells were treated with an iron concentration of 50 μM. This concentration was based on previous published work (Puukila, 2015) (33). Treated cells were incubated for 6 hours, 12 hours, or 24 hours at 37°C. Cell death was assessed after 6 hours of iron treatment, pro-survival protein levels and oxidative stress markers were analysed after 6 and/or 12 hours of iron treatment, and antioxidant levels were assessed after 24 hours. Shorter incubation times were used to determine the effect of acute iron overload on cell signaling proteins.

Secoisolariciresinol diglucoside preparation

SDG (250 or 500 μM) was prepared by dissolving SDG into serum- and antibiotic-free DMEM. H9c2 cells were incubated with SDG for 24 hours prior to iron treatment. SDG was provided by Dr. K. Prasad at the University of Saskatchewan.

Necrosis assay

Necrotic cells were assessed by using Propidium Iodide (PI) stain. After iron treatment, cells were removed from the flasks and centrifuged at 500×g for 5 minutes at room temperature. The supernatant was removed, and cells were washed twice with 1X wash buffer (Sigma-Aldrich, Oakville, ON, Canada). Finally, the cell pellet was resuspended in 400 µL of 1X wash buffer, followed by the addition of 8 µL of PI solution (250 µg m^{-1}). The percentage of PI positive cells was determined by using flow cytometry (BDFACS Calibur flow cytometer).

Mitochondrial membrane potential assay

Mitochondrial membrane potential was measured using the JC-10 assay kit (Sigma-Aldrich; Oakville, ON). A suspension of H9c2 cells (5.0×10^5 cells/well; 3 mL) was seeded onto a 6 well plate and was allowed to adhere overnight. After 24 hours, cells were treated for 6 hours with 50 µM iron solution or serum- and antibiotic-free DMEM. Media was then aspirated and cells were scraped into 500 µL solution containing 5 µL of JC-10 dye per millilitre of assay buffer. Cells were then incubated in the dark for 15 minutes at 37°C. Cells were treated with 30µM FCCP (carbonyl cyanide 4-(trifluoromethoxy) phenylhydrazone) for 30 minutes prior to the JC-10 solution. FCCP depolarises the membrane by transporting protons across the inner mitochondrial membrane and can be used as a positive control for this assay. In apoptotic and necrotic cells, the JC-10 dye forms green fluorescent aggregates in the damaged mitochondria. Aggregates were measured using flow cytometry on channels FL1 and FL2 (Becton Dickinson FACSCalibur flow cytometer).

Western blot

H9c2 cells were disrupted and homogenized in 200 µL of Pathscan buffer (25 mM Tris pH 7.5, 150 mM NaCl, 1 mM EDTA, and 2 mL Triton X made up to 200 mL with distilled water) containing protease inhibitor cocktail (Sigma-Aldrich; Oakville, ON), sodium fluoride and sodium orthovanadate using the Tissuelyser (Qiagen, Redwood City, CA, USA) at 30 Hz for 3 minutes. Cell debris was removed by centrifugation at 8,000xg for 10 minutes at 4°C. Protein content was determined using the DC protein assay following manufacturer's protocol (Bio-Rad Laboratories, Inc., Hercules, CA, USA). For each sample, 30 µg of protein was boiled at 95°C for 5 minutes in loading buffer and subjected to SDS-page electrophoresis. Proteins were transferred to a nitrocellulose membrane using a Trans-blot apparatus (Bio-Rad, Mississauga, ON, Canada). The membrane was blocked with 5% BSA for active proteins or 5% milk for non-active proteins for 1 hour at room temperature. The membrane was then incubated with the appropriate antibody overnight at 4°C. Following washing in 1X Tween-Tris buffered saline (TBST; pH 7.4), the membrane was incubated with the appropriate horseradish peroxidase (HRP)- conjugated secondary antibody for 1 hour at room temperature. Finally, the membrane was washed in 1X TBST, and protein expression was visualized using enhanced chemiluminescence reagent. Following chemiluminescent imaging, membranes were stripped and re-blotted accordingly. All antibodies were purchased from Cell Signaling Technologies (Danvers, MA, USA) except for anti-4-Hydroxynonenal (4HNE) which was purchased from Abcam (Abcam; Cambridge, MA), β-actin was purchased from Santa Cruz Biotechnology (Santa Cruz, CA, USA), and catalase from Sigma (Sigma-Aldrich; Oakville, ON). The dilutions of the antibodies were as follows:

anti-AMPK (1:1000), anti-pAMPK (1:500), anti-Akt (1:1000), anti-pAkt (1:250), anti-mTOR (1:1000), anti-pmTOR (1:500), anti-STAT3 (1:1000), anti-pSTAT3 (1:1000), anti-catalase (1:1000), anti-mnSOD (1:1000), anti-4HNE (1:1000), and β-actin (1:5000). Anti-rabbit IgG (1:1000; Cell Signaling Technologies) secondary antibody was used for all primary antibodies except for mTOR, catalase, and β-actin which used anti-mouse IgG (1:1000, 1:5000 and 1:5000, respectively; Cell Signaling Technologies).

Statistical analysis

Data are presented as the mean ± standard error of the mean (SEM). Data was analyzed using the one-way analysis of variance (ANOVA) followed by Tukey's post-hoc test for multiple comparisons (GraphPad Prism 6 software; San Diego, CA). Comparisons with p-values less than or equal to 0.05 were considered significant.

Results

Effect of SDG on iron-induced necrosis in H9c2 cardiomyocytes

Iron-induced necrosis was investigated in cultured H9c2 cells by using a propidium iodine (PI) stain and mean fluorescence was measured using flow cytometry. Six hours of 50 μM iron treatment caused a significant increase (81.8%) in necrotic cells compared to the untreated control condition as shown in Figure 5-A as a shift in fluorescence intensity. Necrotic cells were reduced (24.3%) after 24-hour pre-treatment with 500 μM SDG, as indicated by increased mean FL1 fluorescence versus the iron alone treatment, although this decrease was not statistically significant (Figure 5-B).

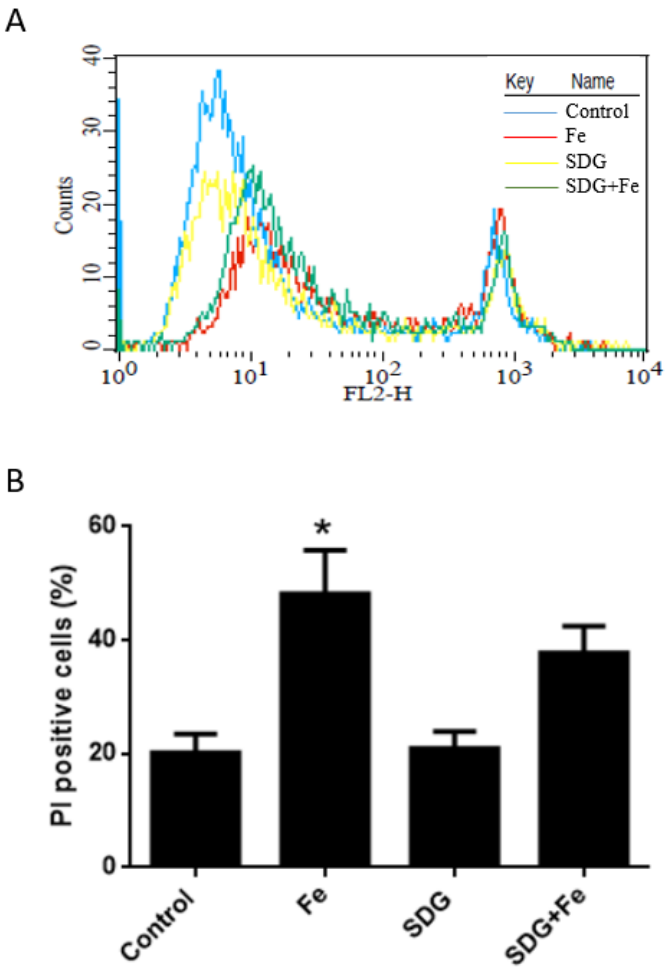

Figure 5: Effect of iron and SDG on necrosis. Depicts PI staining of necrotic cells in control, 50 µM iron (Fe) treated, 500 µM secoisolariciresinol diglucoside (SDG) treated and SDG + Fe treated H9c2 cells. Cells were treated with SDG for 24 hours followed by 6 hours of Fe treatment. Mean fluorescence intensity was measured using flow cytometry. Data was expressed as percent PI positive cells (* = $p \leq 0.05$ vs control/Fe; n=6).

Effect of iron and SDG on mitochondrial membrane potential

Changes in the mitochondrial membrane potential were measured using the JC-10 assay. JC-10 dye accumulates in the mitochondria of healthy cells forming fluorescent red aggregates, however in apoptotic and necrotic cells JC-10 dye will remain in monomeric form fluorescing green. The ratio between green (lower right quadrant) to red (upper right quadrant) determines change in mitochondrial membrane potential (Figure 6-A). Fluorescence was measured using flow cytometry. After 6 hours of iron treatment, there was a decrease (55.6%) in mitochondrial membrane potential compared to the control but this difference was not statistically significant. However, 24-hour pre-treatment of SDG prior to iron treatment caused a statistically significant decrease (55.8%) in damaged mitochondria (Figure 6-B).

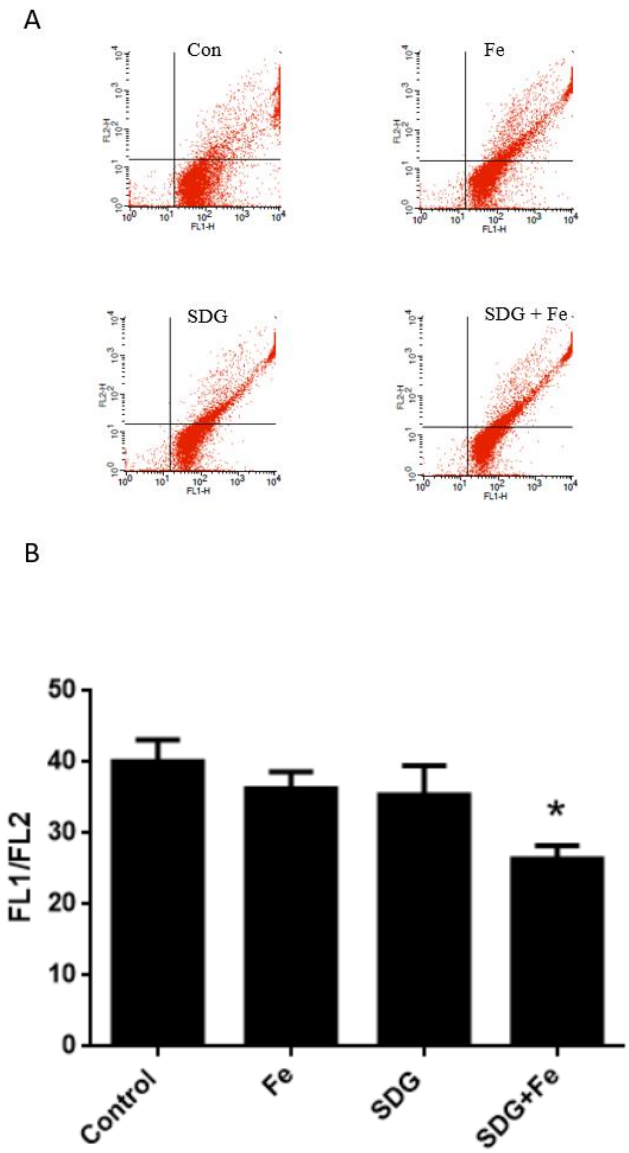

Figure 6: Effect of iron and SDG on the mitochondrial membrane potential. Mitochondrial membrane potential was measured using the JC-10 assay. Mean fluorescence intensity was measured using flow cytometry (A). A ratio between healthy and apoptotic cells was calculated for control, 50 µM iron (Fe) treated, 500 µM secoisolariciresinol diglucoside (SDG) treated and SDG + Fe treated groups (B). Data was expressed as mean fluorescence intensity, arbitrary units (a.u.) (* = $p \leq 0.05$ vs control; n=3)

Effect of iron and SDG on 4HNE

Immunoblotting was used to investigate the effect of iron and SDG on the oxidative stress marker, 4HNE. 4HNE can result in multiple bands on a Western blot depending how it is cleaved by proteases after being released from the membrane. All protein bands present on the membrane were used to measure 4HNE protein content. 4HNE was significantly increased after 6 hours of iron treatment and was also increased in the SDG treated cells compared to control. SDG treatment prior to iron treatment prevented the increase in 4HNE (Figure 7).

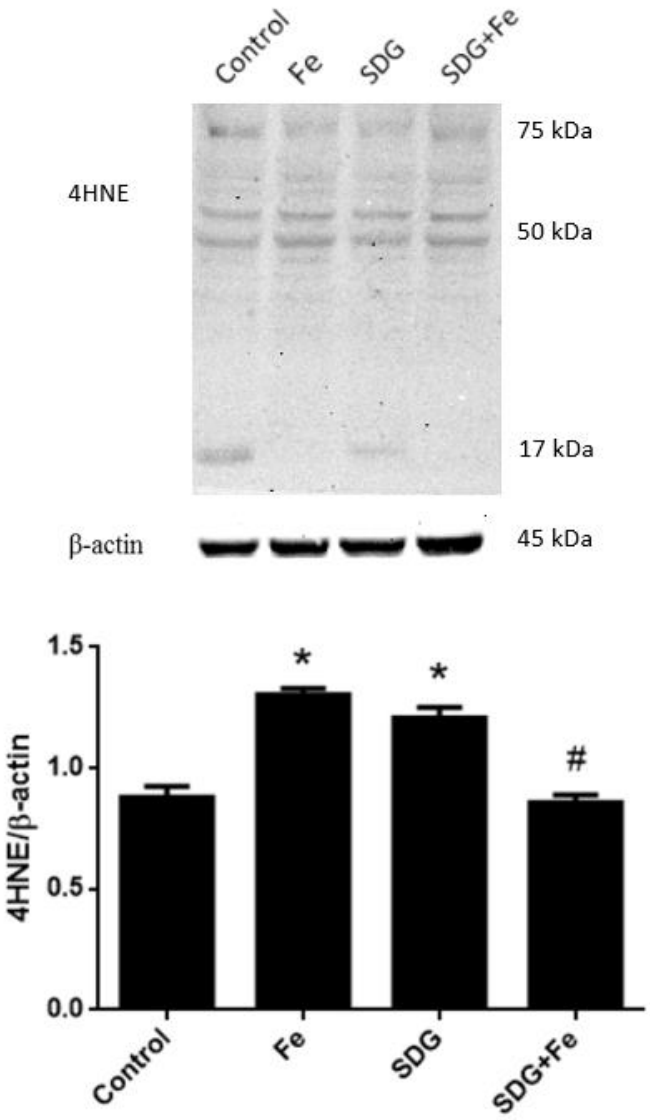

Figure 7: Effect of iron and SDG on 4HNE protein expression. Protein expression of 4HNE in control, 50 μM iron (Fe) treated, 250 μM secoisolariciresinol diglucoside (SDG) treated and SDG + Fe treated H9c2 cells. Cells were treated with SDG for 24 hours and Fe for 6 hours. Protein expression was determined using Western blot and data is expressed as a ratio to β-actin (*/# = $p \leq 0.05$ vs control/Fe; *n*=8).

Effect of iron and SDG on MnSOD and catalase protein expression

To investigate the effect of iron and SDG on antioxidant protein expression, MnSOD and catalase, immunoblotting was performed. After 24 hours of iron treatment there was no significant difference in the amount of MnSOD or catalase compared to control (Figure 8-A, B). However, in cells treated with both SDG and iron, there was a significant increase in the amount of catalase compared to control and iron overload conditions (Figure 8-B).

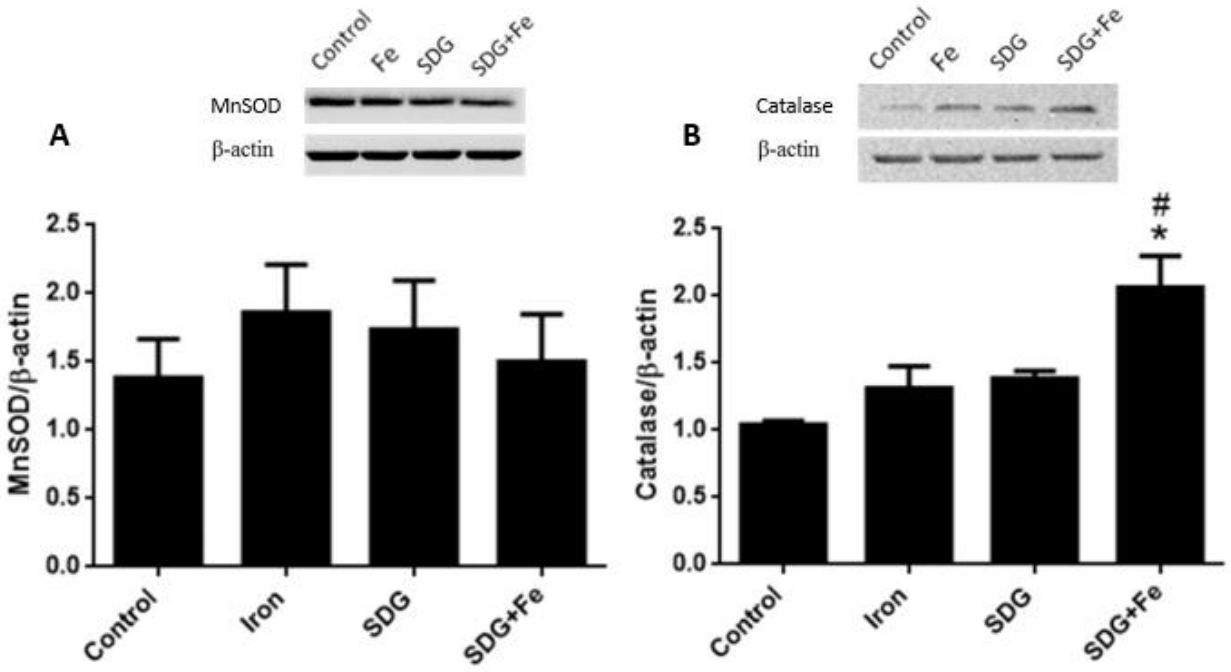

Figure 8: Effect of iron and SDG on antioxidant protein expression. Protein expression of MnSOD (A), and catalase (B) in control, 50 μM iron (Fe) treated, 250 μM secoisolariciresinol diglucoside (SDG) treated and SDG + Fe treated H9c2 cells. Cells were treated with SDG for 24 hours and Fe for 24 hours. Protein expression was determined using Western blot and data is expressed as a ratio to β-actin (*/# = $p \leq 0.05$ vs control/Fe; *n*=5).

Effect of iron and SDG on Akt activity

To further investigate the effect of iron and SDG on intrinsic pro-survival signaling pathways, the activity of Akt was measured using immunoblotting. To determine the amount of active protein in each treatment, a ratio is measured between the active and non-active forms of Akt. After 6 hours of iron treatment, Akt activity was significantly decreased in SDG treated and the combination treatment (Figure 9). Iron alone had no effect on Akt activity.

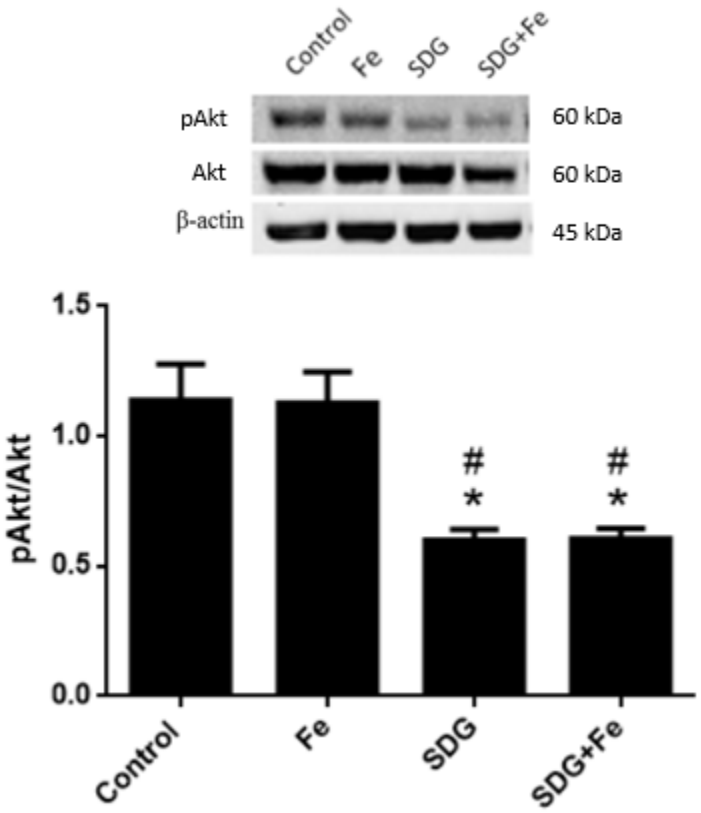

Figure 9: Effect of iron and SDG on Akt activity. Akt activity after 6 hours of iron (Fe) treatment in control, 50 μM Fe treated, 250 μM secoisolariciresinol diglucoside (SDG) treated and SDG + Fe treated H9c2 cells. Protein was determined using Western blot and data was recorded as ratio of active protein to total protein (*/# = $p \leq 0.05$ vs control/Fe respectively; n=3).

Effect of iron and SDG on AMPK activity

AMPK activity was measured using immunoblotting. After 6 hours of iron treatment there was no significant difference noted between any of the conditions (Figure 10-A). However, after 12 hours of iron treatment AMPK activity was increased in the combination treatment but this difference was not found to be significant compared to control and iron overload condition (Figure 10-B). There was an increase between the 12 and 6 hour iron treatment in the combination group.

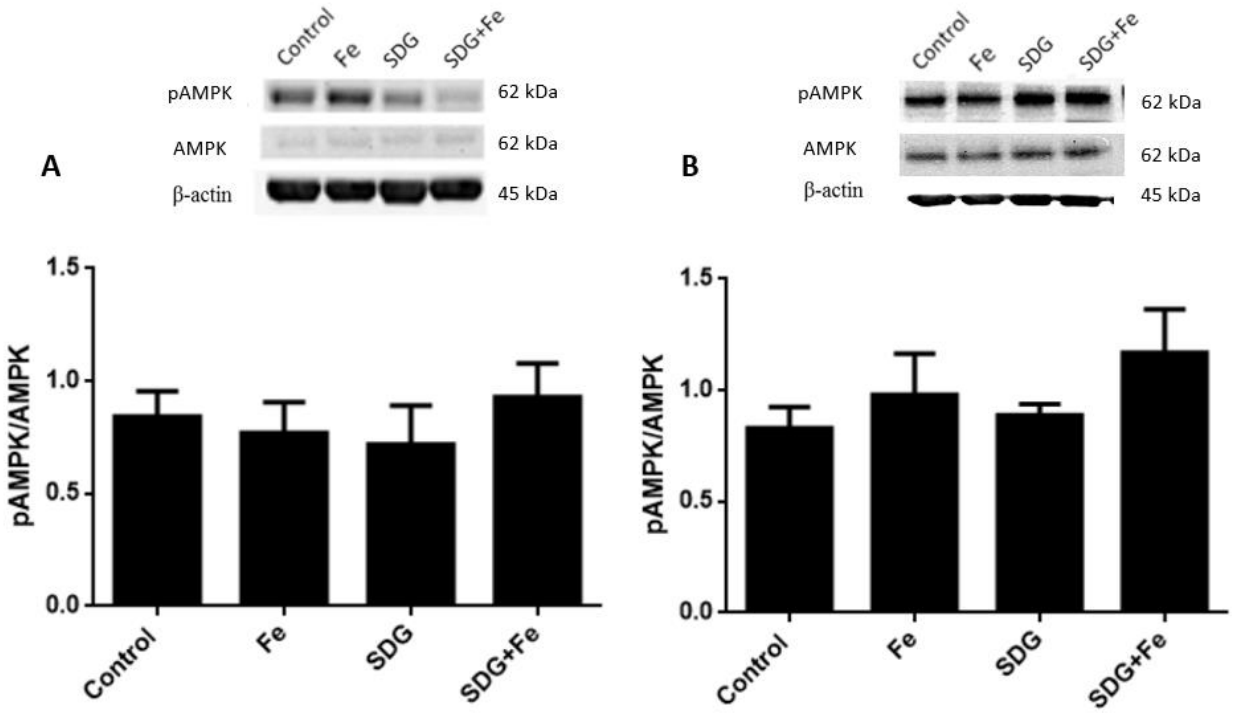

Figure 10: Effect of iron and SDG on AMPK activity. AMPK activity after 6 hours of iron (Fe) treatment (A) and AMPK activity after 12 hours of Fe treatment (B). AMPK activity was shown in control, 50 μM Fe treated, 250 μM secoisolariciresinol diglucoside (SDG) treated and SDG + Fe treated H9c2 cells. Protein was determined using Western blot and data was reported as a ratio of active protein to total protein (*n*=6).

Effect of iron and SDG on mTOR activity

Immunoblotting was used to determine the activity of the protein mTOR. After 6 hours of iron treatment there was no significant difference between conditions (Figure 11-A) as well as after 12 hours of iron treatment (Figure 11-B).

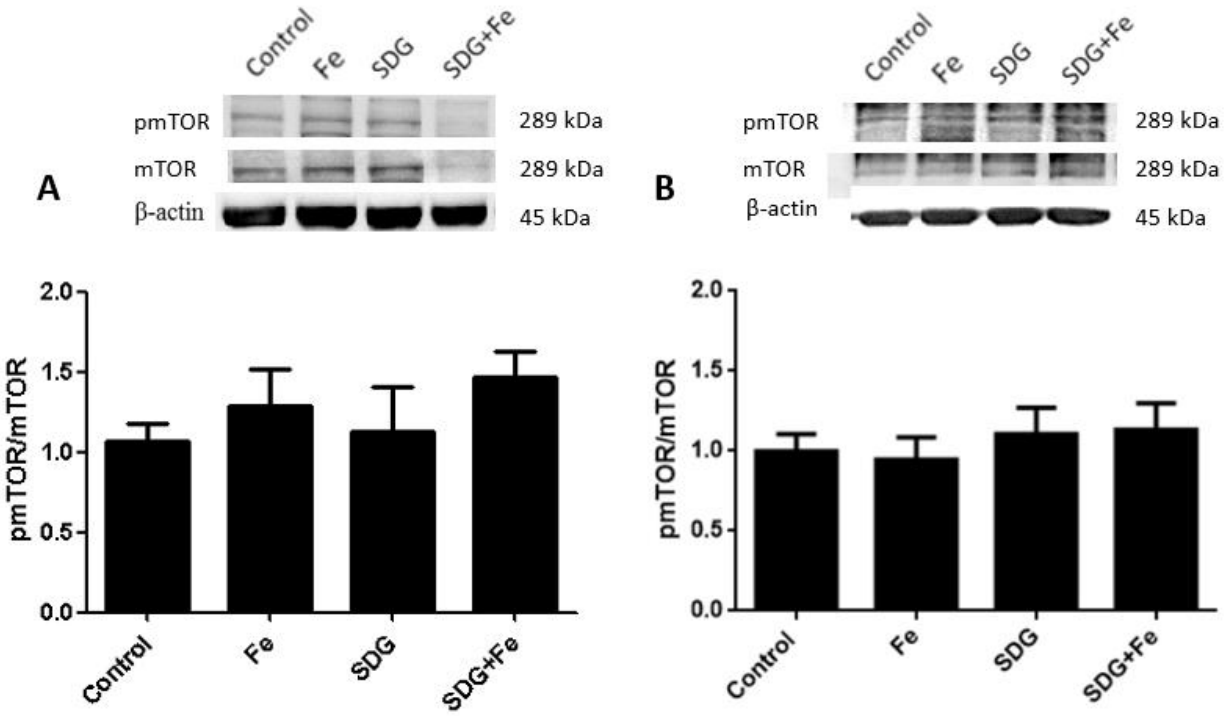

Figure 11: Effect of iron and SDG on mTOR activity. mTOR activity after 6 hours of iron (Fe) treatment (A) and mTOR activity after 12 hours of Fe treatment (B). mTOR activity was shown in control, 50 μM Fe treated, 250 μM secoisolariciresinol diglucoside (SDG) treated and SDG + Fe treated H9c2 cells. Protein was determined using Western blot and data was recorded as a ratio of active protein to total protein (*n*=3).

Effect of iron and SDG on STAT3

The activity of the transcription factor STAT3 was measured using Western blot technique. After 12 hours of iron treatment, STAT3 activity was significantly reduced in comparison to the control. Pre-treatment with SDG increased STAT3 activity but the increase was not significantly different from iron alone (Figure 12).

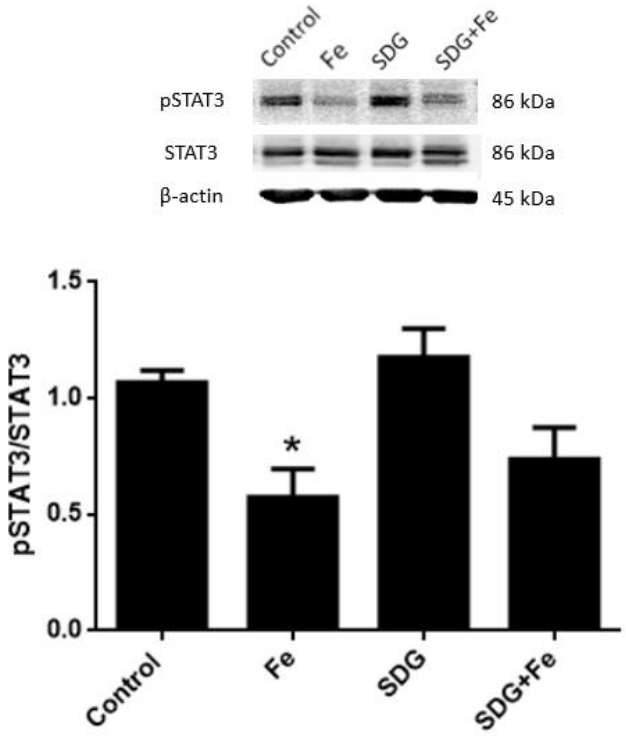

Figure 12: Effect of iron and SDG on STAT3 activity. STAT3 activity after 12 hours of iron (Fe) treatment was assessed via Western blot. STAT3 activity was measured in control, 50 μM Fe treated, 250 μM secoisolariciresinol diglucoside (SDG) treated and SDG + Fe treated H9c2 cells. Data was reported as a ratio of phosphorylated protein to total protein (* = $p \leq 0.05$ vs control/Fe respectively; n=3).

Discussion

Iron overload cardiomyopathy is responsible for substantial cardiovascular morbidity and mortality (1, 2). Oudit et al (2006), demonstrated that free iron in the plasma enters cardiomyocytes via L-type Ca^{2+} channels as reduced iron (2). Fe^{2+} can then lead to the formation of ROS via the Fenton reaction by interacting with ROS produced in the electron transport chain in the mitochondria, interconverting between Fe^{2+} and Fe^{3+} to further generate ROS (Figure 2). Currently the only treatment options for iron overload are phlebotomy or chelation therapy, where both treatments can cause adverse effects. SDG is an antioxidant present in flaxseed and has been shown to decrease the production of inflammatory mediators and ROS. A recent study demonstrated that SDG abrogated the iron-induced increase in oxidative stress, inflammation, and apoptosis (33). For this study, we investigated the effects of iron overload on cell necrosis, antioxidant status, and AMPK signaling in H9c2 cardiac cells. A range of time points were used for iron exposure to determine which proteins in this signaling pathway are activated by short (6 hour) or long (12 or 24 hour) iron exposure. Since cellular protection by SDG is dose dependent, two concentrations of SDG were used (250 μM and 500 μM).

Iron overload in H9c2 cells resulted in an increase in necrosis as measured via flow cytometry. Necrosis is a form of cell death characterized by the permeability changes in the inner mitochondrial membrane resulting in the rupture of the outer mitochondrial membrane releasing proteases into the cytosol (16). PI is a non-membrane permeable dye that can enter into damaged cells and bind to their DNA. In our study, PI positive cells were increased after 6 hours of 50 μM iron treatment and were rescued by 500 μM pretreatment of SDG (Figure 5). This result suggests that iron overload increases

necrosis in H9c2 cells and SDG can reduce the amount of necrotic cells most likely due to its oxidant scavenging properties.

Iron-mediated damage likely involves the role of mitochondrially generated ROS. Previous studies demonstrated that iron overload causes progressive loss of intact mtDNA, decreased expression of respiratory chain subunits encoded by mitochondrial, but not nuclear, DNA, and diminished respiratory function (38, 40, 44, 46). They also reported that iron-mediated cytotoxicity involves ROS generated by the mitochondrion itself because cells lacking mtDNA are remarkably tolerant of iron overload (38). Chan et al (2015) also demonstrated that iron overload decreased the mitochondrial membrane potential (44). JC-10 dye will accumulate in the mitochondrial matrix where it forms red fluorescent aggregates in healthy cells, but in apoptotic and necrotic cells, JC-10 exists in monomeric form and fluoresces green. In our study, iron treated cells had no difference in the ratio of JC-aggregates to monomers between the control group after 6 hours of iron treatment, but showed an increase in the ratio of JC-aggregates to monomers in the SDG + iron treated group compared to the control group (Figure 6). We would expect to see an increase in green monomers in the iron treated group since the mitochondria are a main target for iron induced oxidative stress damage. This result may be because acute iron exposure may not be sufficient to cause mitochondrial damage or the concentration of iron may be too low to elicit a response. Further studies are required to determine the effect of chronic iron overload on the mitochondrial membrane potential.

Overproduction of ROS causes oxidative damage in the cell including lipid peroxidation (15). Lipid peroxidation is the process of free radicals stealing electrons from lipids in cell membranes and the most stable bioactive lipid peroxidation product is

4HNE (15). Previous studies have demonstrated that 4HNE caused an increase in cell death and proteasome activity in H9c2 cardiac cells (49-50). After iron treatment, 4HNE was significantly increased compared to the control and pretreatment of the cardiac cells while SDG attenuated the iron-induced increase in this oxidative stress marker (Figure 7). However, 4HNE concentration was also increased in the SDG condition, suggesting high concentrations of this compound under physiological conditions may negatively regulate oxidative stress. These data suggest SDG has the ability to reduce oxidative stress in iron overload condition.

Antioxidants scavenge ROS to achieve cellular redox balance. We investigated the protein content of MnSOD, which is an antioxidant that catalyzes the reduction of $O_2^{\bullet-}$ to H_2O_2 and O_2, and catalase, which promotes the conversion of H_2O_2 to H_2O and O_2. Bartfay et al (1999) reported that iron overload decreased antioxidant defenses and increased ROS in a murine model (39, 51). Previous work in our lab demonstrated SOD activity was significantly increased in the SDG + iron combination condition and SDG alone treatment compared to iron and control treatments (33). In our study, iron treatment increased the SOD protein expression as well as in the SDG treatment but the SDG + iron treated cardiac cells reduced SOD to control levels (Figure 8-A). Discrepancies between previous study may be due to different concentrations of SDG treatment. Catalase was significantly increased when cells were treated with both SDG and iron (Figure 8-B). This data suggests that SDG can boost intrinsic antioxidant activity in iron overload condition.

The Akt/mTOR pathway is a pro-survival pathway that is involved in many cellular processes including autophagy, cell growth, and transcription of cellular

metabolites such as antioxidants (41-42). Wang et al, 2011, showed chronic iron overload in a gerbil model reduced the activity of Akt (41). In our study, after acute iron exposure, there was no difference between the iron and control condition, but SDG significantly reduced the activity of Akt compared to the iron and control cells (Figure 10). Dikshit et al (2016), demonstrated SDG reduced the expression of Akt in hens. These data suggest SDG has an effect on Akt protein and gene expression (43).

AMPK, a downstream target of Akt, reserves cellular energy status and serves as a key regulator of cell survival in response to energy stress. No significant difference was found in AMPK activity after 6 or 12 hours of iron treatment. However, Puukila et al (2015) showed a decrease in AMPK expression after 24 hours of iron treatment. This suggests a chronic iron exposure may affect AMPK activity (33). SDG pretreatment increased the activity of AMPK after iron overload suggesting AMPK may be targeted by SDG to provide protection against iron-induced oxidative stress. mTOR is a downstream target of AMPK and regulates a number of cellular processes including autophagy and cell growth. mTOR activity was not affected by iron or SDG suggesting that after acute iron exposure mTOR is not altered by SDG and iron (Figure 11). Further experiments need to be conducted to determine if the Akt-mTOR pathway is a key player in protection against iron overload and if the activity of Akt is related to the production of catalase after SDG exposure.

The STAT3 transcription factor has been shown to have an impact on cardiomyocyte survival by regulating genes involved in anti-oxidative pathways, modulation of hypertrophic growth, angiogenesis, and metabolic reserves (37, 47-48). STAT3 has been shown to up-regulate MnSOD in mice thereby suppressing ROS

accumulation (37, 45). After iron treatment, STAT3 activity was significantly reduced compared to the control cells (Figure 12). Pre-treatment with SDG increased the activity of STAT3, but this was not significantly different from the control cells. This increase may result in the activation of antioxidant proteins, such as catalase whose expression was increased due to SDG treatment.

Using H9c2 cardiac cells exposed to iron overload condition, we demonstrated an increase in cell death, antioxidants, and decrease in STAT3. This was observed by measuring cell death, antioxidant protein expression, and cell survival proteins. SDG abrogated the increase in cellular damage and the reduction of prosurvival proteins, further confirming the cardioprotective role for SDG in cardiac iron overload. However, further experiments are required to determine the effect of this condition on Akt/mTOR signaling.

Limitations

This study was limited by using an *in vitro* model instead of an *in vivo* model of cardiac iron overload and as such the results should be extrapolated accordingly. Markers of cell survival and oxidative stress were studied by only measuring protein expression, further enzyme activity assays and gene expression analysis should be performed to gain an in-depth understanding of the role of SDG in cardiac iron overload.

Conclusion

Cardiac iron overload directly correlates with cardiac dysfunction and may ultimately cause heart failure. Cardiac dysfunction is likely caused by a combination of oxidative stress and inflammation, which can lead to cell death. SDG is an antioxidant phytoestrogen present in flax seeds that has been shown to prevent the development of hypercholesterolemic atherosclerosis and diabetes. Here we investigated the role of SDG on markers of cell death, mitochondrial dysfunction, and pro-survival signaling. The results of these *in vitro* studies demonstrated that H9c2 rat cardiac cell were susceptible to iron overload, as demonstrated by increased necrosis and mitochondrial damage. Pre-treatment with SDG abrogated the detrimental effects of iron overload, suggesting a possible role for SDG as a cardioprotective agent in iron overload condition.

References

1) Feng, Z. (2010). p53 Regulation of the IGF-1/AKT/mTOR Pathways and the Endosomal Compartment. *Cold Spring Harbor Perspectives in Biology*, *2*(2), a001057.
2) Oudit, G. Y., Trivieri, M. G., Khaper, N., Liu, P. P., & Backx, P. H. (2006). Role of L-Type Ca2+ Channels in Iron Transport and Iron-Overload Cardiomyopathy. *Journal of Molecular Medicine*, *84*(5), 349-364.
3) Gujja, P., Rosing, D. R., Tripodi, D. J., & Shizukuda, Y. (2010). Iron Overload Cardiomyopathy: Better Understanding of an Increasing Disorder. *Journal of the American College of Cardiology*, *56*(13), 1001-1012.
4) Britton, R. S., Leicester, K. L., & Bacon, B. R. (2002). Iron Toxicity and Chelation Therapy. *International Journal of Hematology*, *76*(3), 219-228.
5) Prasad, K. (1997). Hydroxyl Radical-Scavenging Property of Secoisolariciresinol Diglucoside (SDG) Isolated from Flax-Seed. *Molecular and Cellular Biochemistry*, *168*(1-2), 117-123.
6) Andrews, N. C. (1999). Disorders of Iron Metabolism. *The New England Journal of Medicine, 341*(26), 1986-1995.
7) Shander, A., Cappellini, M.D., & Goodnough, L.T. (2009). Iron Overload and Toxicity: The Hidden Risk of Multiple Blood Transfusions. *Vox Sanguinis, 97*(3), 185-197.
8) Murphy, C. J., & Oudit, G. Y. (2010). Iron-Overload Cardiomyopathy: Pathophysiology, Diagnosis, and Treatment. *Journal of Cardiac Failure*, *16*(11), 888-900.

9) McBride, M. (2004). Strategies to Reduce Oxidative Stress in Cardiovascular Disease. *Clinical Science*, *106*, 219-234.

10) Venkataraman, K., Khurana, S., & Tai, T. C. (2013). Oxidative Stress in Aging-Matters of the Heart and Mind. *International Journal of Molecular Sciences*, *14*(9), 17897-17925.

11) Papaharalambus, C. A., & Griendling, K. K. (2007). Basic Mechanisms of Oxidative Stress and Reactive Oxygen Species in Cardiovascular Injury. *Trends in Cardiovascular Medicine*, *17*(2), 48-54.

12) Cachofeiro, V., Goicochea, M., de Vinuesa, S. G., Oubiña, P., Lahera, V., & Luño, J. (2008). Oxidative Stress and Inflammation, a Link Between Chronic Kidney Disease and Cardiovascular Disease. *Kidney International*, *74*, S4-S9.

13) Battin, E. E., & Brumaghim, J. L. (2009). Antioxidant Activity of Sulfur and Selenium: A Review of Reactive Oxygen Species Scavenging, Glutathione Peroxidase, and Metal-Binding Antioxidant Mechanisms. *Cell Biochemistry and Biophysics*, *55*(1), 1-23.

14) Flora, S. J. (2009). Structural, Chemical and Biological Aspects of Antioxidants for Strategies Against Metal and Metalloid Exposure. *Oxidative Medicine and Cellular Longevity*, *2*(4), 191-206.

15) Zhong, H., & Yin, H. (2015). Role of Lipid Peroxidation Derived 4-Hydroxynonenal (4-HNE) in Cancer: Focusing on mitochondria. *Redox Biology*, *4*, 193-199.

16) Mughal, W., Dhingra, R., & Kirshenbaum, L. A. (2012). Striking a Balance: Autophagy, Apoptosis, and Necrosis in a Normal and Failing Heart. *Current Hypertension Reports*, *14*(6), 540-547.

17) Essick, E. E., & Sam, F. (2010). Oxidative Stress and Autophagy in Cardiac Disease, Neurological Disorders, Aging and Cancer. *Oxidative Medicine and Cellular Longevity*, *3*(3), 168-177.

18) Xie, Z., & Klionsky, D. J. (2007). Autophagosome Formation: Core Machinery and Adaptations. *Nature Cell Biology*, *9*(10), 1102-1109.

19) Gurusamy, N., & Das, D. K. (2009). Autophagy, Redox Signaling, and Ventricular Remodeling. *Antioxidants & Redox Signaling*, *11*(8), 1975-1988.

20) Martinet, W., Knaapen, M. W., Kockx, M. M., & De Meyer, G. R. (2007). Autophagy in Cardiovascular Disease. *Trends in Molecular Medicine*, *13*(11), 482-491.

21) Dong, Y., Undyala, V. V., Gottlieb, R. A., Mentzer, R. M., & Przyklenk, K. (2010). Review: Autophagy: Definition, Molecular Machinery, and Potential Role in Myocardial Ischemia-Reperfusion Injury. *Journal of Cardiovascular Pharmacology and Therapeutics*, *15*(3), 220-230.

22) Gottlieb, R. A., & Mentzer Jr, R. M. (2010). Autophagy During Cardiac Stress: Joys and Frustrations of Autophagy. *Annual Review of Physiology*, *72*, 45.

23) Shao, D., Oka, S. I., Liu, T., Zhai, P., Ago, T., Sciarretta, S., ... & Sadoshima, J. (2014). A Redox-Dependent Mechanism for Regulation of AMPK Activation by Thioredoxin1 During Energy Starvation. *Cell Metabolism*, *19*(2), 232-245.

24) Li, X. N., Song, J., Zhang, L., LeMaire, S. A., Hou, X., Zhang, C., ... & Shen, Y. H. (2009). Activation of the AMPK-FOXO3 Pathway Reduces Fatty Acid–Induced Increase in Intracellular Reactive Oxygen Species by Upregulating Thioredoxin. *Diabetes*, *58*(10), 2246-2257.

25) Xie, Z., He, C., & Zou, M. H. (2011). AMP-Activated Protein Kinase Modulates Cardiac Autophagy in Diabetic Cardiomyopathy. *Autophagy*, *7*(10).

26) Paiva, M. A., Rutter-Locher, Z., Gonçalves, L. M., Providência, L. A., Davidson, S. M., Yellon, D. M., & Mocanu, M. M. (2011). Enhancing AMPK Activation During Ischemia Protects the Diabetic Heart Against Reperfusion Injury. *American Journal of Physiology-Heart and Circulatory Physiology*, *300*(6), H2123-H2134.

27) Kasznicki, J., Sliwinska, A., & Drzewoski, J. (2014). Metformin in Cancer Prevention and Therapy. *Annals of Translational Medicine*, *2*(6), 57.

28) Gurusamy, N., & Das, D. K. (2009). Autophagy, Redox Signaling, and Ventricular Remodeling. *Antioxidants & Redox Signaling*, *11*(8), 1975-1988.

29) Feng, Z., Hu, W., De Stanchina, E., Teresky, A. K., Jin, S., Lowe, S., & Levine, A. J. (2007). The Regulation of AMPK β1, TSC2, and PTEN Expression by p53: Stress, Cell and Tissue Specificity, and the Role of these Gene Products in Modulating the IGF-1-AKT-mTOR Pathways. *Cancer Research*, *67*(7), 3043-3053.

30) Marsh, J., Mukherjee, P., & Seyfried, T. N. (2008). Akt-Dependent Proapoptotic Effects of Dietary Restriction on Late-Stage Management of a Phosphatase and

Tensin Homologue/Tuberous Sclerosis Complex 2–Deficient Mouse Astrocytoma. *Clinical Cancer Research*, *14*(23), 7751-7762.

31) Feng, Z. (2010). p53 Regulation of the IGF-1/AKT/mTOR Pathways and the Endosomal Compartment. *Cold Spring Harbor Perspectives in Biology*, *2*(2), a001057.

32) Prasad, K. (2009). Flaxseed and Cardiovascular Health. *Journal of Cardiovascular Pharmacology*, *54*(5), 369-377.

33) Puukila, S., Bryan, S., Laakso, A., Abdel-Malak, J., Gurney, C., Agostino, A., ... & Khaper, N. (2015). Secoisolariciresinol Diglucoside Abrogates Oxidative Stress-Induced Damage in Cardiac Iron Overload Condition. *PloS One*, *10*(3), e0122852.

34) Adolphe, J. L., Whiting, S. J., Juurlink, B. H., Thorpe, L. U., & Alcorn, J. (2010). Health Effects with Consumption of the Flax Lignan Secoisolariciresinol Diglucoside. *British Journal of Nutrition*, *103*(07), 929-938.

35) Prasad, K. (1997). Hydroxyl Radical-Scavenging Property of Secoisolariciresinol Diglucoside (SDG) Isolated from Flax-Seed. *Molecular and Cellular Biochemistry*, *168*(1-2), 117-123.

36) Hu, C., Yuan, Y. V., & Kitts, D. D. (2007). Antioxidant Activities of the Flaxseed Lignan Secoisolariciresinol Diglucoside, its Aglycone Secoisolariciresinol and the Mammalian Lignans Enterodiol and Enterolactone In Vitro. *Food and Chemical Toxicology*, *45*(11), 2219-2227.

37) Haghikia, A., Stapel, B., Hoch, M., & Hilfiker-Kleiner, D. (2011). STAT3 and Cardiac Remodeling. *Heart Failure Reviews*, *16*(1), 35-47.

38) Gao, X., Campian, J. L., Qian, M., Sun, X. F., & Eaton, J. W. (2009). Mitochondrial DNA Damage in Iron Overload. *Journal of Biological Chemistry*,*284*(8), 4767-4775.

39) Bartfay, W. J., Butany, J., Lehotay, D. C., Sole, M. J., Hou, D., Bartfay, E., & Liu, P. P. (1999). A Biochemical, Histochemical, and Electron Microscopic Study on the Effects of Iron-Loading on the Hearts of Mice. *Cardiovascular Pathology*, *8*(6), 305-314.

40) Pucheu, S., Coudray, C., Tresallet, N., Favier, A., & De Leiris, J. (1993). Effect of Iron Overload in the Isolated Ischemic and Reperfused Rat Heart. *Cardiovascular Drugs and Therapy*, *7*(4), 701-711.

41) Otto-Duessel, M., Aguilar, M., Moats, R., & Wood, J. C. (2007). Antioxidant-Mediated Effects in a Gerbil Model of Iron Overload. *Acta haematologica*,*118*(4), 193-199.

42) Wang, Y., Wu, M., Al-Rousan, R., Liu, H., Fannin, J., Paturi, S., ... & Triest, W. E. (2011). Iron-Induced Cardiac Damage: Role of Apoptosis and Deferasirox Intervention. *Journal of Pharmacology and Experimental Therapeutics*,*336*(1), 56-63.

43) Dikshit, A., Gao, C., Small, C., Hales, K., & Hales, D. B. (2016). Flaxseed and its Components Differentially Affect Estrogen Targets in Pre-Neoplastic Hen Ovaries. *The Journal of Steroid Biochemistry and Molecular Biology*, *159*, 73-85.

44) Chan, S. H. I. N. G., Chan, G. C., Ye, J., Lian, Q., Chen, J., & Yang, M. (2015). Thrombopoietin Protects Cardiomyocytes from Iron-Overload Induced Oxidative

Stress and Mitochondrial Injury. *Cellular Physiology and Biochemistry*, *36*(5), 2063-2071.

45) Wang, Y., Wang, D., Zhang, L., Ye, F., Li, M., & Wen, K. (2016). Role of JAK-STAT Pathway in Reducing Cardiomyocytes Hypoxia/Reoxygenation Injury Induced by S1P Postconditioning. *European Journal of Pharmacology*, *784*, 129-136.

46) Nanayakkara, G., Alasmari, A., Mouli, S., Eldoumani, H., Quindry, J., McGinnis, G., ... & Amin, R. (2015). Cardioprotective HIF-1α-Frataxin Signaling Against Ischemia-Reperfusion Injury. *American Journal of Physiology-Heart and Circulatory Physiology*, *309*(5), H867-H879.

47) Hilfiker-Kleiner, D., Kaminski, K., Podewski, E., Bonda, T., Schaefer, A., Sliwa, K., ... & Luchtefeld, M. (2007). A Cathepsin D-Cleaved 16 kDa Form of Prolactin Mediates Postpartum Cardiomyopathy. *Cell*, *128*(3), 589-600.

48) Kurdi, M., & Booz, G. W. (2009). JAK Redux: A Second Look at the Regulation and Role of JAKs in the Heart. *American Journal of Physiology-Heart and Circulatory Physiology*, *297*(5), H1545-H1556.

49) Mali, V. R., Deshpande, M., Pan, G., Thandavarayan, R. A., & Palaniyandi, S. S. (2016). Impaired ALDH2 Activity Decreases the Mitochondrial Respiration in H9C2 Cardiomyocytes. *Cellular Signalling*, *28*(2), 1-6.

50) Deshpande, M., Mali, V. R., Pan, G., Xu, J., Yang, X. P., Thandavarayan, R. A., & Palaniyandi, S. S. (2016). Increased 4-Hydroxy-2-Nonenal-Induced Proteasome Dysfunction is Correlated with Cardiac Damage in Streptozotocin-

Injected Rats with Isoproterenol Infusion. *Cell Biochemistry and Function*, *34*(5), 334-342.

51) McCullough, K. D., & Bartfay, W. J. (2007). The Dose-Dependent Effects of Chronic Iron Overload on the Production of Oxygen Free Radicals and Vitamin E Concentrations in the Liver of a Murine Model. *Biological Research for Nursing*, *8*(4), 300-304.

52) Carnero, A., Blanco-Aparicio, C., Renner, O., Link, W., & Leal, J. F. (2008). The PTEN/PI3K/AKT Signalling Pathway in Cancer, Therapeutic Implications. *Current Cancer Drug Targets*, *8*(3), 187-198.

53) Gammella, E., Recalcati, S., Rybinska, I., Buratti, P., & Cairo, G. (2015). Iron-Induced Damage in Cardiomyopathy: Oxidative-Dependent and Independent Mechanisms. *Oxidative Medicine and Cellular Longevity*, *2015*.